

Predominant 1,2-Insertion of Styrene in the Pd-Catalyzed Alternating Copolymerization with Carbon Monoxide

Kyoko Nozaki,^{*,†} Hatsumi Komaki,[†] Yasutoyo Kawashima,[†] Tamejiro Hiyama,[†] and Toshiaki Matsubara^{*,‡}

Contribution from the Department of Material Chemistry, Graduate School of Engineering, Kyoto University, Sakyo-ku, Kyoto 606-8501 Japan, and Institute for Fundamental Chemistry, Takano-Nishihiraki-cho, Sakyo-ku, Kyoto 606-8103, Japan

Received April 21, 2000

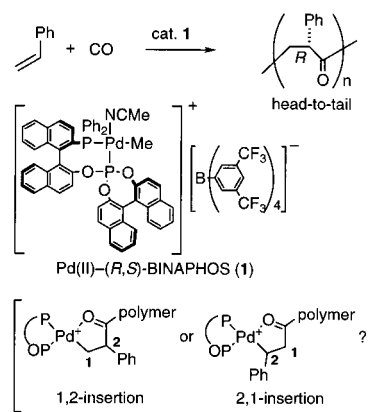
Abstract: The regioselectivity of styrene insertion to an acyl–Pd bond was studied by NMR in (i) a stoichiometric reaction and (ii) a copolymerization with CO. In the stoichiometric reaction of styrene with [(CH₃CO)Pd(CH₃CN){(R,S)-BINAPHOS}]·[B{3,5-(CF₃)₂C₆H₃}]₄, both 1,2- and 2,1-products were given. To mimic the real polymerization conditions, a polyketone-substituted complex [(CH₃(CH₂CHCH₃CO)_n]Pd{(R,S)-BINAPHOS}·[B{3,5-(CF₃)₂C₆H₃}]₄ (*n* ≈ 14) was prepared. When this polymer-attached Pd species was treated with styrene, the 1,2-insertion product was the only detectable species. Thus, exclusive 1,2-insertion is demonstrated to be responsible for the styrene–CO copolymerization, in sharp contrast to the predominant 2,1-insertion with conventional nitrogen ligands. Chain-end analysis revealed that β-hydride elimination took place from the 2,1-complex but not from the 1,2-complex. Thus, once 2,1-insertion occurs, rapid β-hydride elimination proceeds to terminate the polymerization, as is common to the other phosphorus–ligand systems. The resulting Pd–H species re-initiates the copolymerization, as was proven by MALDI-TOF mass analysis of the product copolymers.

Introduction

The regioselectivity of α-olefin insertion to a metal–carbon bond, either primary (1,2-insertion) or secondary (2,1-insertion), is known to depend on both the nature of olefins and the metal complexes. Complete 2,1-insertion is reported for the alternating copolymerization of styrene with carbon monoxide¹ when the reaction is initiated by Pd(II) complexes of 1,10-phenanthroline,² 2,2'-bipyridyl,³ a bisoxazoline,⁴ and other bidentate sp² nitrogen ligands.⁵ Only one example was reported for possible 1,2-insertion by Consiglio and co-workers employing phosphine–oxazoline ligands.⁶ In their studies, larger substituents in the phosphine part raised the proportion of the 1,2-insertion, and as a result, regioirregular copolymers were obtained.

In contrast to the nitrogen-based ligands, phosphines have been known as undesirable ligands for the alternating copolymerization of styrene with CO.^{1b,5c} When Pd(*p*-CH₃C₆H₄SO₃)₂-

Scheme 1



(1,3-bisdiphenylphosphinopropane) was employed as a catalyst, rapid β-hydride elimination is claimed to have followed the 2,1-insertion of styrene, affording mainly dimers but not polymers.² Unlike other phosphorus ligands, (R,S)-BINAPHOS gave a copolymer of 4-*tert*-butylstyrene and CO, and thus, enantioselective alternating copolymerization has been achieved.^{7,8} Here we reveal that exclusive 1,2-insertion is responsible for the styrene–CO copolymerization with Pd-(R,S)-BINAPHOS (Scheme 1, Figure 1). This unique regioselectivity is suggested to explain why a regiocontrolled alternating copolymer was obtained with this particular phosphorus ligand. When 2,1-insertion takes place, rapid β-hydride elimination occurs, as is

(7) (a) Nozaki, K.; Sato, N.; Takaya, H. *J. Am. Chem. Soc.* **1995**, *117*, 9911. (b) Nozaki, K.; Sato, N.; Tonomura, Y.; Yasutomi, M.; Takaya, H.; Hiyama, T.; Matsubara, T.; Koga, N. *J. Am. Chem. Soc.* **1997**, *119*, 12779.

(8) Nozaki, K.; Kawashima, Y.; Nakamoto, K.; Hiyama, T. *Macromolecules* **1999**, *32*, 5168.

[†] Kyoto University.

[‡] Institute for Fundamental Chemistry.

(1) Alternating copolymerization of styrene with CO: (a) Drent, E. Eur. Pat. Appl. 1986, 229408; *Chem. Abstr.* **1988**, *108*, 6617. Reviews: (b) Drent, E. *Chem. Rev.* **1996**, *96*, 663. (c) Sen, A. *Acc. Chem. Res.* **1993**, *26*, 303. (d) Nozaki, K.; Hiyama, T. *J. Organomet. Chem.* **1999**, *576*, 248.

(2) Barsacchi, M.; Consiglio, G.; Medici, L.; Petrucci, G.; Suster, U. *W. Angew. Chem., Int. Ed. Engl.* **1991**, *30*, 989.

(3) Brookhart, M.; Rix F. C.; DeSimone, J. M.; Barborak, J. C. *J. Am. Chem. Soc.* **1992**, *114*, 5894.

(4) Bartolini, S.; Carfagna, C.; Musco, A. *Macromol. Rapid Commun.* **1995**, *16*, 9.

(5) (a) Carfagna, C.; Formica, M.; Gatti, G.; Musco, A.; Pierleoni, A. *Chem. Commun.* **1998**, 1113. (b) Milani, B.; Anzilutti, A.; Vicentini, L.; Santi, A. S.; Zangrando, E.; Geremia, S.; Mestroni, G. *Organometallics* **1997**, *16*, 5064. (c) Milani, B.; Paronetto, F.; Zangrando, E. *J. Chem. Soc., Dalton Trans.* **2000**, *18*, 3055.

(6) (a) Sperrle, M.; Aeby, A.; Consiglio, G.; Pfaltz, A. *Helv. Chim. Acta* **1996**, *79*, 1387. (b) Aeby, A.; Gsponer, A.; Consiglio, G. *J. Am. Chem. Soc.* **1998**, *120*, 11000. (c) Aeby, A.; Bangerter, F.; Consiglio, G. *Helv. Chim. Acta* **1998**, *81*, 764.

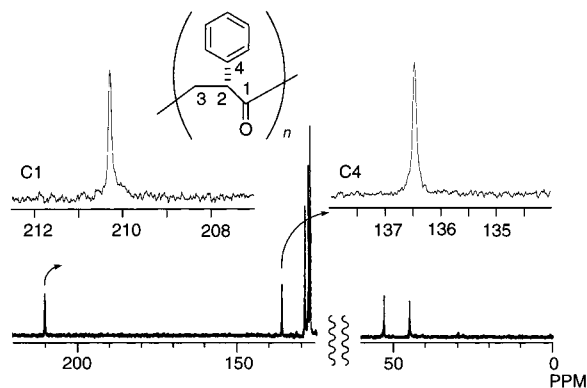


Figure 1. ^{13}C NMR (CDCl_3) peaks of poly(styrene-*alt*-CO) obtained with **1**. The peaks due to carbonyl C1 (left) and ipso C4 are enlarged. Almost complete regioselectivity and isotactic selectivity are estimated by comparison of these two peaks with those in ref 6b. The configuration of the asymmetric carbon is determined to be *R* on the basis of optical rotation and ref 11.

common with the other phosphorus ligands, to terminate the polymerization.

Results and Discussion

1. Studies on the Initial Styrene Insertion in the Alternating Copolymerization. Species from Acetylplatinum-(*R,S*)-BINAPHOS and Styrene. Acetylplatinum **2**, prepared from methylplatinum **1**, was treated with styrene, and the reaction was monitored by ^{31}P NMR (Figure 2). The observations are summarized in Scheme 2. Characterization of complexes **3a–c**, **4**, and **8a,b** is described in the next paragraph. First, 3 molar equivalents of styrene was added to a solution of acetylplatinum **2** in CDCl_3 at -10°C . After 3 h at this temperature, two alkylplatinum species appeared: a 1,2-insertion product, complex **3a**, and a 2,1-insertion product, complex **4** (Figure 2(i)). When the sample was kept at -10°C for another 1 h and then at 20°C for 3 h, acetylplatinum **2** gradually converted into 1,2-complexes **3a–c** and 2,1-complex **4** (Figure 2(ii)). Complexes **3b** and **3c** are diastereomers of **3a**. In **3b**, the alkyl group is *cis* to the phosphine, while the alkyl group is *trans* to the phosphine in **3a**. The opposite enantioface of styrene is selected in **3c** compared to **3a**. In Figure 2(ii), formation of π -benzylplatinum complexes **8a,b** is also detectable. Complexes **8a** and **8b** are, again, diastereomers to each other that originate from the selection of the two enantiofaces of styrene. After another 41 h at 20°C , both complexes **3** and **4** disappeared and π -benzylplatinum complexes **8a,b** became the only visible species (Figure 2(iii)). At this stage, olefin protons due to 3-phenyl-3-buten-2-one (**5**) and 4-phenyl-3-buten-2-one (benzalacetone, **6**) were detected by ^1H NMR. Thus, the observations above can be summarized as follows. Styrene insertion to acetylplatinum **2** takes place both in 1,2- and 2,1-fashions to give complexes **3a–c** and **4**, both of which undergo the β -hydride elimination to release the corresponding α,β -unsaturated ketones **5** and **6**, respectively. Meanwhile, the Pd–H species **7** thus prepared reacts with styrene to form benzyl complexes **8a,b**.

Characterization of Complexes 3a–c, 4, and 8a,b. Complexes **3a–c**, **4**, and **8a,b** were characterized as follows, occasionally by ^{13}C -labeling either the terminal carbon of styrene ($\text{PhCH}=\text{}^{13}\text{CH}_2$) or carbon monoxide (^{13}CO). Representative results are summarized in Figure 3. In complex **3a**, the chemical shift and $J_{\text{P–C}}$ values of the coordinated ketone, δ 237.7 ($J_{\text{P}^{\text{a}}\text{–C}} = 11$ Hz and $J_{\text{P}^{\text{b}}\text{–C}} = 2.4$ Hz, where P^{a} represents the phosphorus atom of the phosphine and P^{b} that of the phosphite), are close to the reported values for the propene-inserted complex

9a.^{7b} The chemical shift and $J_{\text{P–C}}$ values for the carbon that comes from C-2 of styrene, δ 39.3 ($J_{\text{P}^{\text{a}}\text{–C}} = 80$ Hz and $J_{\text{P}^{\text{b}}\text{–C}} = 6.1$ Hz), also match the values for dodecene-inserted complex **10a.**^{7b} Thus, the structure of **3a** was determined. For the other two 1,2-complexes, **3b** and **3c**, the $J_{\text{P–C}}$ between the terminal carbon of styrene and the two phosphorus atoms of **3b** and **3c** are quite close to those of **10b** and **10a**, respectively. The data for the coordinated ketones of **3b** and **3c** correspond to those of **9b** and **9a**. Furthermore, the chemical shift and $J_{\text{P–P}}$ in ^{31}P NMR of **3b** and **3c** (see Experimental Section) are similar to those of **9b** and **9a**, respectively. All these data together enabled us to assign the structures of **3b** and **3c**. Characterization of **4** and **8a** (and **8b**) follows the reports on their corresponding Pd–1,10-phenanthroline complexes **11** and **12**, respectively. In complex **4**, the chemical shifts for the carbons from C-2 of styrene (δ 51.8) and from ^{13}CO (δ 224.1) both match the ones in the Pd–1,10-phenanthroline complex **11** reported by Brookhart et al.³ The coupling constants $J_{\text{P–C}} = 12$, 3.6 Hz observed in the carbonyl carbon are common to **3a** and **9a**. In complexes **8a** and **8b**, chemical shifts for the carbons originating from styrene C-2, δ 16.2 and 18.5, respectively, are similar to the value for π -benzyl complex **12** with 1,10-phenanthroline.⁹ ^{13}C NMR (DEPT) manifested that the carbons are CH_3 . Labeling CO with carbon-13 did not affect the ^{31}P NMR peaks, suggesting that CO is included in neither **8a** nor **8b**. Thus, **8a** and **8b** are characterized as diastereomers of π -benzyl complex, selecting the opposite enantioface of π -benzyl to bind to Pd. Although the formation of Pd enolate **13** was anticipated,¹⁰ none of the ^{13}C NMR peaks was assignable to the oxygen-attached carbon, which would exhibit its peak at around δ 188.0 in the ^{13}CO experiment.

Carbomethoxylation of Complexes 3, 4, and 8 to Esters 14–16. Carbomethoxylation of the Pd–C bond of complexes **3**, **4**, and **8** afforded the corresponding esters. After treatment of **2** with styrene at 20°C for 2 h, the solution of complexes **3a–c**, **4**, **8a,b**, and **1** ($\text{3a–c/4/8a,b/1} = 48/20/16/16$) was allowed to react with MeOH and CO to give esters **14**, **15**, and **16** corresponding to **3**, **4**, and **8**, as shown in Scheme 3.^{6a} Characterization of esters **14** and **15** is described in the next paragraph. Benzalacetone (**6**), which was given by the β -hydride elimination from complex **4**, was also obtained in 4% yield. Here, it should be noted that the *S*-isomers were the major enantiomers in **14**, **15**, and **16**, in sharp contrast to the *R*-configuration of the asymmetric carbon in the copolymer main chain.

Characterization of Esters 14 and 15. Authentic samples of esters **14** and **15** were synthesized as a racemic mixture (Schemes 4 and 5). Treatment of (*E*)-3-phenyl-2-propen-1-ol (cinnamyl alcohol, **17**) with trimethyl orthoformate and acid gave methyl 3-phenyl-4-pentenoate (**18**) via Claisen rearrangement. Wacker oxidation of the β,γ -unsaturated ester **18** provided ester **14**. Ester **15** was derived from the corresponding β,γ -unsaturated ester **21** via Wacker oxidation. Esters **14** and **15** were hydrolyzed to their corresponding carboxylic acids **19** and **22** and resolved with optically pure (*R*)-1-phenylethylamine and

(9) Rix, F. C.; Brookhart, M.; White, P. S. *J. Am. Chem. Soc.* **1996**, *118*, 2436.

(10) Zuideveld, M. A.; Kamer, P. C. J.; van Leeuwen, P. W. N. M.; Klusener, P. A. A.; Stil, H. A.; Roobeek, C. F. *J. Am. Chem. Soc.* **1998**, *120*, 7977.

(11) Bartolini, S.; Carfagna, C.; Musco, A. *Macromol. Rapid. Commun.* **1995**, *16*, 9.

(12) Mosher, H. S.; Clark, D. R. *J. Org. Chem.* **1970**, *35*, 1114.

(13) Cookson, R. C.; Kemp, J. E. *Chem. Commun.* **1971**, 385.

(14) The analysis described in this paragraph was suggested by one of the referees in the reviewing process. We are deeply indebted to the referee for the helpful comment.

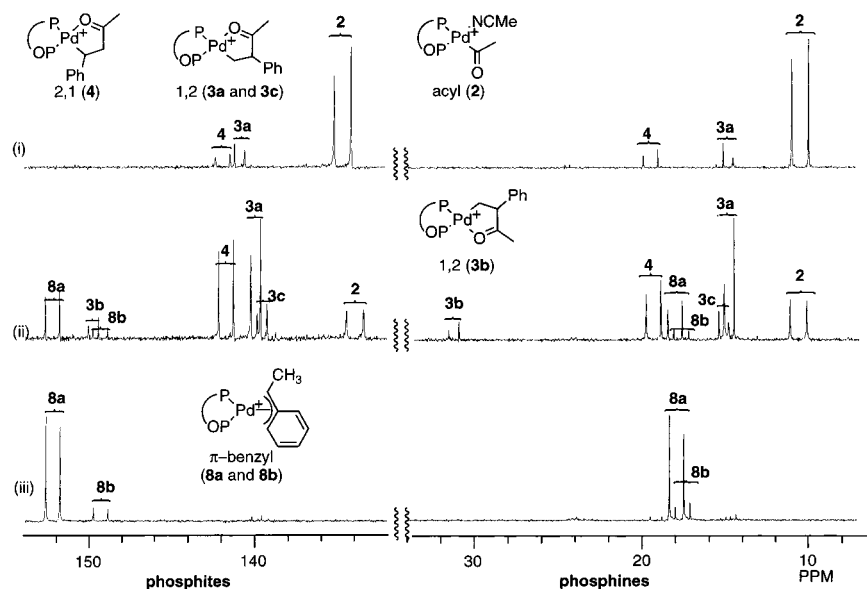
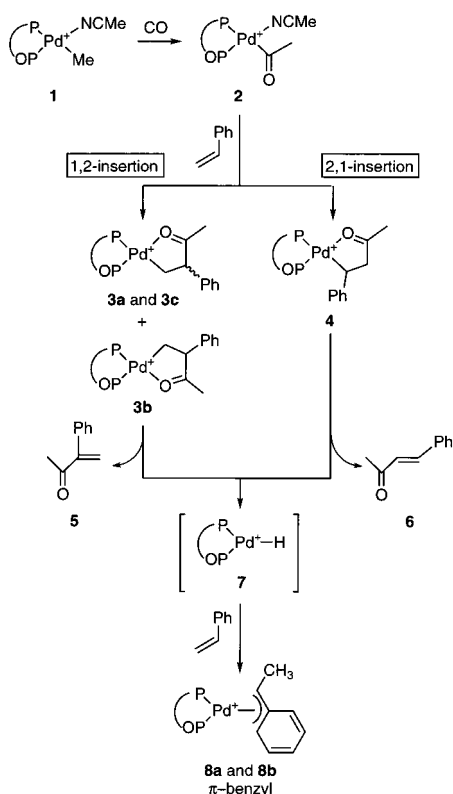


Figure 2. ^{31}P NMR studies on the styrene insertion to acylpalladium **2**. Phosphines exhibit peaks within δ 7–34 and phosphites within δ 132–154. All the peaks are observed as doublets due to their phosphorus–phosphorus couplings between the phosphine and the phosphite parts. (i) -10 $^{\circ}\text{C}$, 3 h: In addition to acyl complex **2**, 1,2-insertion product **3a** and 2,1-insertion product **4** appeared. (ii) -10 $^{\circ}\text{C}$, 4 h; 20 $^{\circ}\text{C}$ 3 h: One more major new species, π -benzylic complex **8a**, appeared. At the same time, three more minor species were also detected: **3b** and **3c** (diastereomers of **3a**), and **8b** (a diastereomer of **8a**). The peak for the phosphite in **3a** upfield-shifted by 1.0 ppm depending on the temperature. (iii) -10 $^{\circ}\text{C}$, 4 h; 20 $^{\circ}\text{C}$, 44 h: Finally, π -benzylic complex **8a** and **8b** became the only visible species.

Scheme 2



(*S*)-1-(2-naphthyl)ethylamine, respectively. Optically active acids **19** and **22** thus obtained were esterified again to **14** and **15**. The absolute configuration of each ester was determined by comparing the sign of optical rotation with related compounds as shown in Figure 4. As shown, α -phenyl ketone **23**, β -phenylcarboxylic ester **25**, and β -phenylcarboxylic acid **27**, which have some parts in common with **14** or **19**, are (*S*)-(+). Similarly, compounds **24**, **26**, and **28** corresponding to **15** and **22** are all (*S*)-(+). Thus, here we tentatively determine that compounds

14, **15**, **19**, and **22** possess *S* absolute configuration when the optical rotation sign is plus.

2. Studies on the Styrene Insertion in the Polymer Propagation. Predominant 1,2-Insertion of Styrene into the Polymer-Substituted Acyl–Pd Bond. The contradicting selectivities between the stoichiometric reaction (Schemes 2 and 3) and the copolymerization (Scheme 1) prompted us to investigate the effect of a grown-up polymer chain on the styrene insertion. To mimic the real polymerization process, complex **29** with a polymeric substituent was prepared, taking advantage of the living nature^{7b} of the alternating copolymerization of propene and CO (Scheme 6). First, methylpalladium **1** was treated with propene (3 atm) and CO (20 atm) at 20 $^{\circ}\text{C}$ for 15 min to form alkyl complex **29**. An aliquot of the solution of **29** was quenched by carbomethoxylation, and the degree of polymerization was estimated to be ca. 14 by size exclusion chromatography with polystyrene standard. Alkyl complex **29** thus prepared was treated with styrene (3 molar equivalents to Pd) and CO (20 atm) at -20 $^{\circ}\text{C}$ for 15 h. After the pressure was released, the 1,2-styrene insertion product **30** was detected by ^{31}P NMR analysis at δ 139.8 (d, $J_{\text{P-P}} = 67$ Hz) and 14.3 (d, $J_{\text{P-P}} = 67$ Hz), the values being identical to those for the 1,2-insertion complex **3a** (δ 139.9 (d, $J_{\text{P-P}} = 64$ Hz), 14.6 (d, $J_{\text{P-P}} = 64$ Hz)) (Figure 5). No peaks were assignable to the 2,1-product **31**, which would appear in the region of the 2,1-complex **4** (δ 141.7 (d, $J_{\text{P-P}} = 98$ Hz), 19.1 (d, $J_{\text{P-P}} = 98$ Hz)). With $\text{PhCH}=\text{C}^{13}\text{H}_2$, $J_{\text{P-A-C}} = 80$ Hz was observed for the phosphorus nucleus of the phosphine in **30**. None of the other phosphorus peaks was affected by the ^{13}C labeling. Thus, when the polyketone chain is attached to the palladium center, 1,2-insertion is suggested to be the predominant process for the styrene insertion.

Suggested Reaction Pathways. The results obtained above suggest the following reaction pathways. At the initial stage, the styrene insertion to acetyl palladium takes place with rather low regio- and enantioselectivities, as was revealed with our stoichiometric studies. In contrast, the regiochemistry is strictly controlled when a polymer chain is attached to the Pd center.

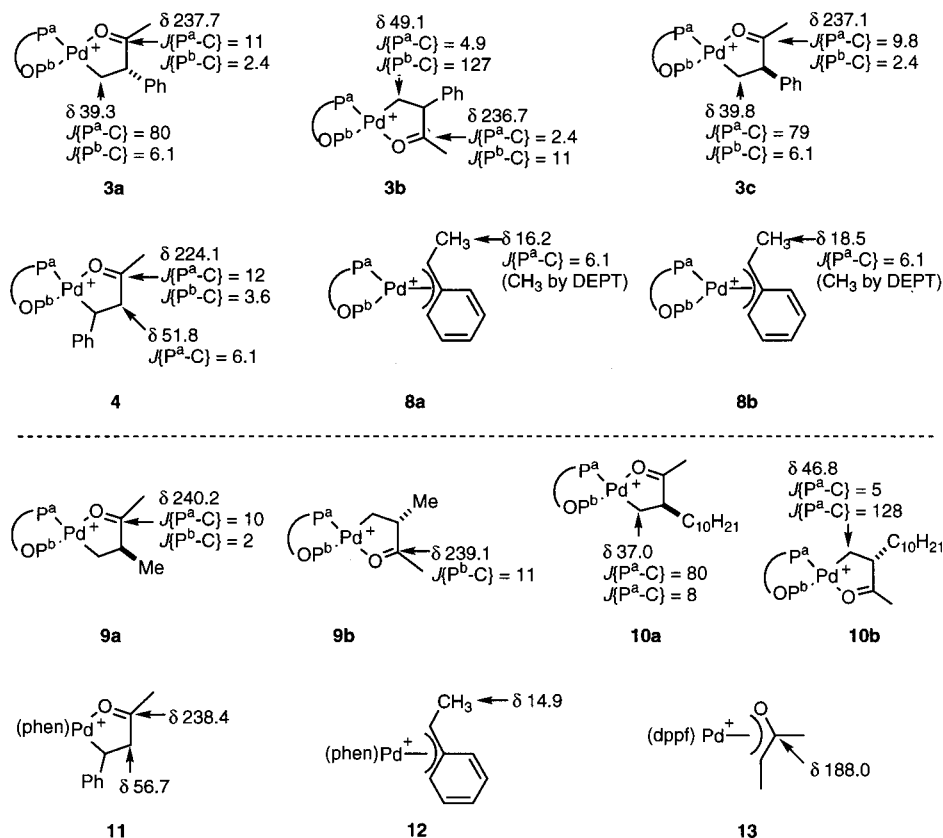
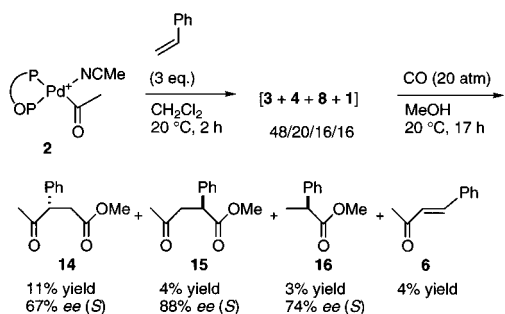
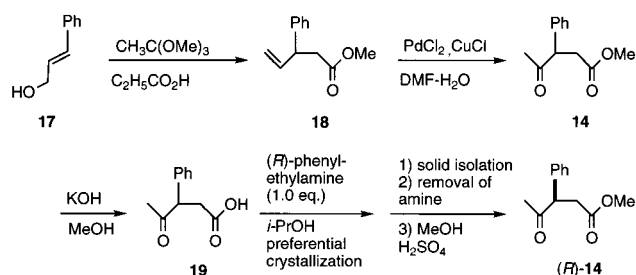


Figure 3. ^{13}C NMR data for characterization of complexes **3a–c**, **4**, and **8a,b** (coupling constants are given in hertz). Complexes **3a–c**, **4**, and **8a,b** were characterized by comparing their data with those of known complexes **9a,b**,^{7b} **10a,b**,^{7b} **11**,³ and **12**.⁹ See text for details. Although the formation of Pd enolate **13** was anticipated,¹⁰ none of the ^{13}C NMR peaks was assignable to the oxygen-attached carbon.

Scheme 3



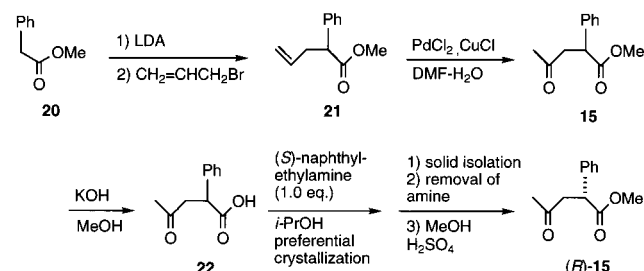
Scheme 4



Since almost complete regioselectivities and isotactic selectivities are estimated by the ^{13}C NMR chart in Figure 1,^{6b} it is likely that styrene insertion predominantly proceeded in a 1,2-fashion since a very early stage of the copolymerization.

3. Chain Termination. The chain end of the copolymer was analyzed by ^1H NMR (Figure 6). Olefinic protons due to the (*E*)-PhCH=CHC(=O)— group were observed, but no *exo*-methylene protons of the $\text{CH}_2=\text{CH}(\text{Ph})\text{C}(\text{=O})—$ group were

Scheme 5



detected. Thus, it is proposed that the chain termination took place exclusively from 2,1-complexes **33**, polymeric analogues of **4**, while chain propagation proceeded from 1,2-complexes **32**, as shown in Scheme 7. The resulting Pd–H species **7** then reacted with styrene to give the π -benzyl complex **8**.

Chain re-initiation by **8** has been demonstrated by MALDI-TOF mass analysis, as shown in Figure 7. Two series of polymers are observed: those attributed to polymer **I**, $\text{CH}_3-(\text{COCHPhCH}_2)_n-\text{COCH}=\text{CHPh}$ (minor), and those attributed to polymer **II**, $\text{Ph}(\text{Me})\text{CH}-(\text{COCHPhCH}_2)_n-\text{COCH}=\text{CHPh}$. The former polymer was initiated by acetyl palladium **2** and the latter by phenethyl palladium **8**. In both polymers, the other ends are phenylethenyl groups resulting from the β -hydride elimination.

On the basis of the above studies, the ratio of 1,2- and 2,1-insertions can be calculated as follows.¹⁴ Because 1,2-insertion causes polymerization and 2,1-insertion results in chain transfer, the ratio of polymerization rate R_p and chain transfer rate R_{ct} can be expressed as $R_p/R_{ct} = k_{1,2}/k_{2,1}$, using the reaction rate $k_{1,2}$ for the 1,2-insertion and $k_{2,1}$ for the 2,1-insertion. The ratio R_p/R_{ct} equals the average degree of polymerization. We meas-

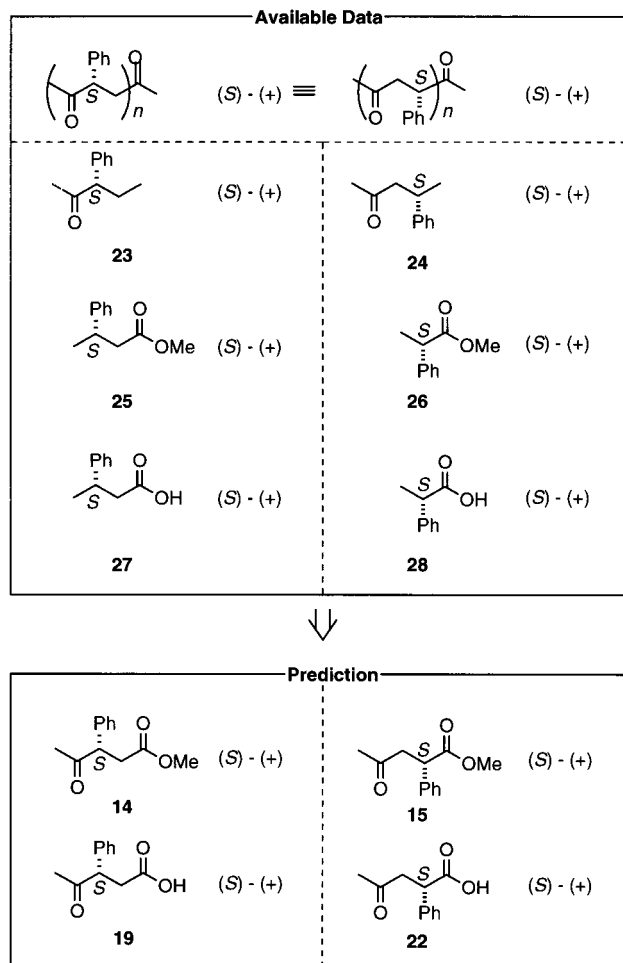
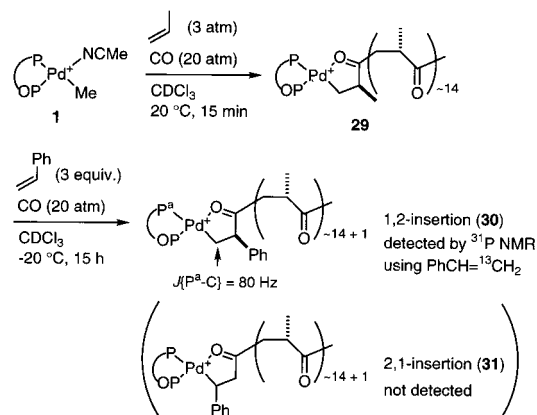


Figure 4. Determination of the absolute configurations of methyl 4-oxo-3-phenylpentanoate (**14**) and methyl 4-oxo-2-phenylpentanoate (**15**). The signs of optical rotation are compared with those of the corresponding ketones and esters. From the top, the absolute configuration of the polyketone was determined by Bartolini et al.¹¹ Other reported values are the following: **23**¹² (*S* pure), $[\alpha]_D +368$ (benzene); **24**¹³ (*R* pure), $[\alpha]_D -74.5$ (benzene); **25**¹³ (*R* pure), $[\alpha]_D -44.3$ (benzene); **26** (*R*, 97% ee was prepared by treatment of (*R*)-2-phenylpropanoic acid (available from Aldrich) with MeOH/H₂SO₄), $[\alpha]_D -85.0$ (CHCl₃); **27**¹³ (*R* pure), $[\alpha]_D -60.0$ (benzene); **28** (*R* pure), $[\alpha]_D -72$ (CHCl₃) available from Aldrich.

Scheme 6



ured the molecular weight to be 1800 based on ¹H NMR, as shown in Figure 6, and thus the polymerization degree value is 1800/132 = ca. 14. This implies that, since the second insertion of styrene, the 1,2/2,1 ratio of insertion is 93/7.

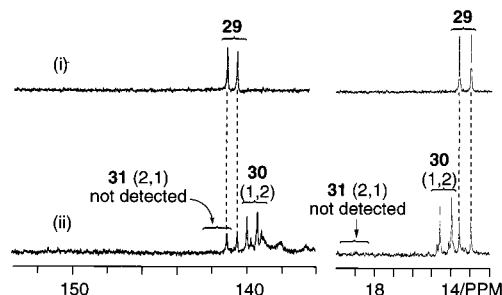


Figure 5. Studies on the styrene insertion to the Pd polymer complex **29**. (i) ³¹P NMR (CDCl₃ at 20 °C) of polymer complex **29**. (ii) After treatment of **29** with styrene under CO at -20 °C for 15 h, 1,2-insertion product **30** appeared but not 2,1-product **31**. The structure of **29** was determined by using PhCH=¹³CH₂ (see Experimental Section).

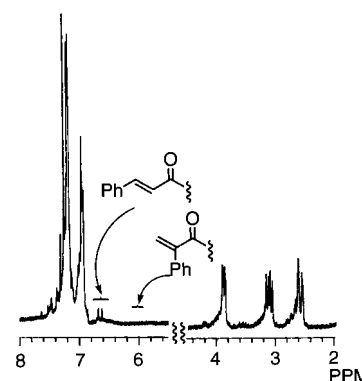


Figure 6. ¹H NMR of poly(styrene-*alt*-CO) obtained with **1**. At δ 6.66, a doublet due to the PhCH=CH-C(=O)- group is shown. On the other hand, no peaks are detectable in the region of δ 5.9–6.2, where *exo*-methylene protons would exhibit peaks if the CH₂=CPh-C(=O)- group existed. On the basis of the integration, the molecular weight of the polymer was calculated to be 1800.

4. Factors Which Control the Regioselectivity of Styrene Insertion: A Theoretical Approach.

Although the factors which control the regioselectivity are not clear at this moment, in this section we propose that the bulky ligand (*R,S*)-BINAPHOS preferred the 1,2-insertion in order to avoid steric repulsion between the ligand and the phenyl group of styrene on the basis of theoretical studies.^{7b,15} In fact, a molecular orbital (MO) calculation with the density functional method (B3LYP) suggested the preferred 2,1-insertion over 1,2 when the phosphine and the phosphite parts of (*R,S*)-BINAPHOS are replaced by PH₃ and P(OH)₃, respectively. Meanwhile, 1,2-insertion is predicted to be more likely by the ONIOM method¹⁶ on a real molecule, especially when a longer chain is attached to the Pd center. Details are as follows.

Preferable 2,1-Insertion in the Model Molecule. To examine the electronic effect of the phenyl group of styrene in the styrene insertion step, we first performed MO calculations at the B3LYP level of density functional theory¹⁷ for its transition state (TS) using the model molecule, where the

(15) (a) Svensson, M.; Matsubara, T.; Morokuma, K. *Organometallics* **1996**, *15*, 5568. (b) Margl, P.; Ziegler, T. *J. Am. Chem. Soc.* **1996**, *118*, 7737. (c) Margl, P.; Ziegler, T. *Organometallics* **1996**, *15*, 5519. (d) Michalak, A.; Ziegler, T. *Organometallics* **2000**, *19*, 1850.

(16) (a) Dapprich, S.; Komáromi, I.; Byun, K. S.; Morokuma, K.; Frish, M. J. *J. Mol. Struct. (THEOCHEM)* **1999**, *461–462*, 1. (b) Humbel, S.; Sieber, S.; Morokuma, K. *J. Chem. Phys.* **1996**, *105*, 1959. (c) Maseras, F.; Morokuma, K. *J. Comput. Chem.* **1995**, *16*, 1170. (d) Matsubara, T.; Sieber, S.; Morokuma, K. *Int. J. Quantum Chem.* **1996**, *60*, 1101. (e) Svensson, M.; Humbel, S.; Froese, R. D. J.; Matsubara, T.; Sieber, S.; Morokuma, K. *J. Chem. Phys.* **1996**, *100*, 19357. (f) Matsubara, T.; Maseras, F.; Koga, N.; Morokuma, K. *J. Chem. Phys.* **1996**, *100*, 2573.

Scheme 7

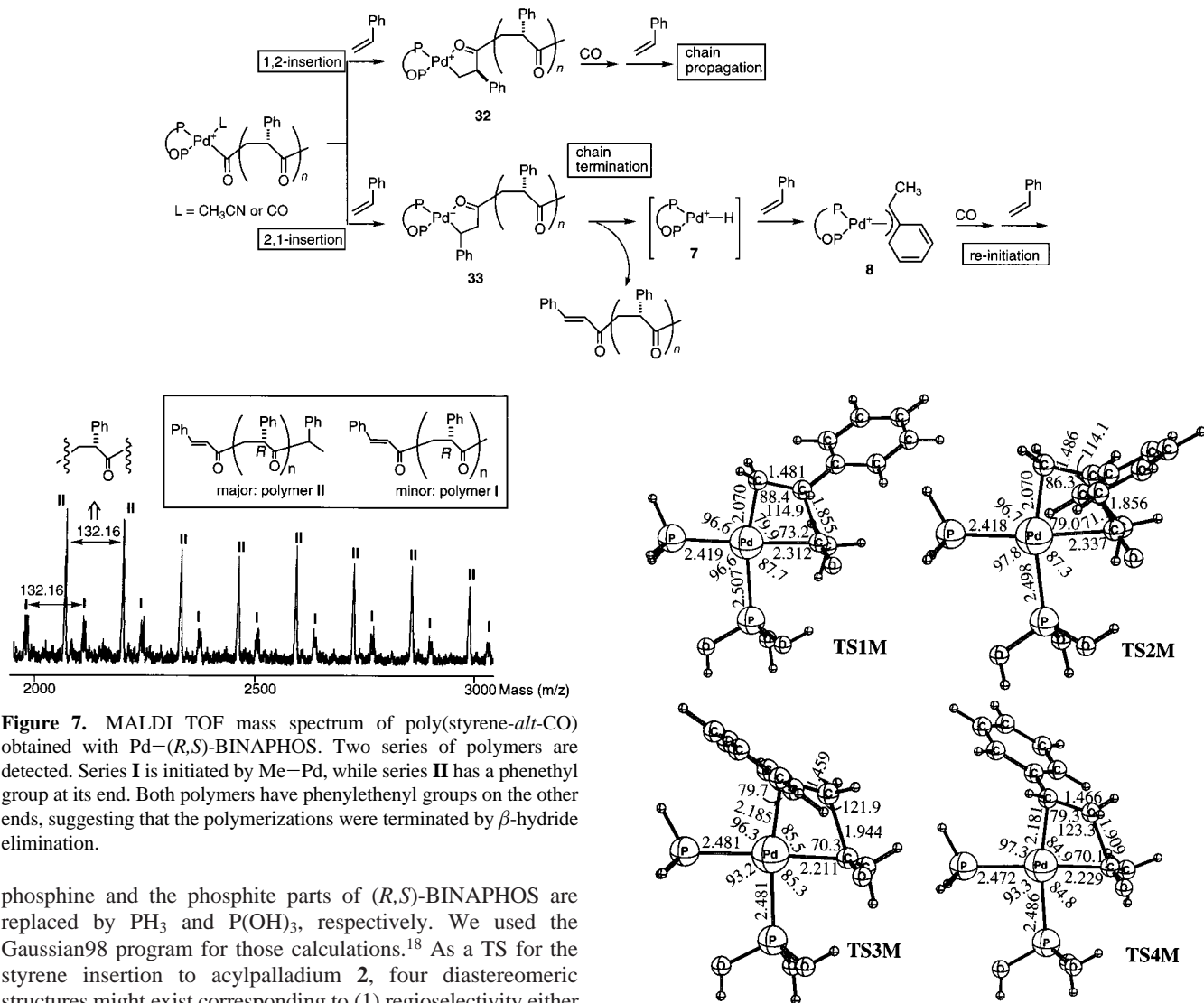


Figure 7. MALDI TOF mass spectrum of poly(styrene-*alt*-CO) obtained with Pd-(*R,S*)-BINAPHOS. Two series of polymers are detected. Series **I** is initiated by Me-Pd, while series **II** has a phenethyl group at its end. Both polymers have phenylethenyl groups on the other ends, suggesting that the polymerizations were terminated by β -hydride elimination.

phosphine and the phosphite parts of (*R,S*)-BINAPHOS are replaced by PH_3 and $\text{P}(\text{OH})_3$, respectively. We used the Gaussian98 program for those calculations.¹⁸ As a TS for the styrene insertion to acylpalladium **2**, four diastereomeric structures might exist corresponding to (1) regioselectivity either for 1,2- or 2,1-insertion and (2) the orientation of the phenyl either syn or anti to the carbonyl oxygen. The structures of those TSs fully optimized at the B3LYP level with the basis set lanl2dz, namely **TS1–4M**, are presented in Figure 8. Those TSs were identified by the number of imaginary frequencies calculated from the analytical Hessian matrix. Our calculation showed that the TSs which have styrene trans to phosphite is more stable in energy by 6–8 kcal/mol than the TSs which have styrene trans to phosphine in the present styrene system, as we reported the same trend in the previous system of the similar model molecule utilizing ethene as the olefin.^{7b} Therefore, in this study, we focused on the TSs, where styrene is

Figure 8. Optimized structures (in Å and deg) of the transition states **TS1–4M** in the 1,2- and 2,1-insertion of styrene into the acetyl-Pd bond with the density functional method (B3LYP/lanl2dz). The model molecule, in which the phosphine and the phosphite parts of (*R,S*)-BINAPHOS are replaced by PH_3 and $\text{P}(\text{OH})_3$, respectively, was used. Transition states for 2,1-insertion, **TS1M** and **TS2M**, showed lower energy values compared to those for 1,2-insertion, **TS3M** and **TS4M**.

trans to phosphite. The electronic effect of the phenyl group of styrene is explicitly reflected in the geometry of the TSs. One will readily notice that the TSs of 2,1-insertion (**TS3M** and **TS4M**) are more reactant-like compared to those of 1,2-insertion (**TS1M** and **TS2M**), since the C=C double bond of olefin and the Pd–C(acyl) bond are shorter and the Pd–C(olefin) and the C(olefin)–C(acyl) bonds are longer. The calculated relative energy showed that **TS3M** and **TS4M** are more stable by 6–7 kcal/mol than **TS1M** and **TS2M**, as presented in Table 1, which suggests that 2,1-insertion is favorable over 1,2-insertion.

Equally Probable 1,2- and 2,1-Insertions in the Real Molecule: The Initial Styrene Insertion. We next investigated the effect of the ligand on the TSs using the real molecule constructed by combining the model molecule with (*R,S*)-BINAPHOS. Here, eight diastereomeric TSs were considered in the real molecule because, in the combination, the enantiomer has to be taken into account for each of four diastereomeric

(17) (a) Becke, A. D. *Phys. Rev. A* **1988**, *38*, 3098. (b) Lee, C.; Yang W.; Parr, R. G. *Phys. Rev. B* **1988**, *37*, 785. (c) Becke, D. J. *Chem. Phys.* **1993**, *98*, 5648.

(18) Frisch, M. J.; Trucks, G. W.; Schlegel, H. B.; Scuseria, G. E.; Robb, M. A.; Cheeseman, J. R.; Zakrzewski, V. G.; Montgomery, J. A., Jr.; Stratmann, R. E.; Burant, J. C.; Dapprich, S.; Millam, J. M.; Daniels, A. D.; Kudin, K. N.; Strain, M. C.; Farkas, O.; Tomasi, J.; Barone, V.; Cossi, M.; Cammi, R.; Mennucci, B.; Pomelli, C.; Adamo, C.; Clifford, S.; Ochterski, J.; Petersson, G. A.; Ayala, P. Y.; Cui, Q.; Morokuma, K.; Malick, D. K.; Rabuck, A. D.; Raghavachari, K.; Foresman, J. B.; Cioslowski, J.; Ortiz, J. V.; Stefanov, B. B.; Liu, G.; Liashenko, A.; Piskorz, P.; Komaromi, I.; Gomperts, R.; Martin, R. L.; Fox, D. J.; Keith, T.; Al-Laham, M. A.; Peng, C. Y.; Nanayakkara, A.; Gonzalez, C.; Challacombe, M.; Gill, P. M. W.; Johnson, B.; Chen, W.; Wong, M. W.; Andres, J. L.; Gonzalez, C.; Head-Gordon, M.; Replogle, E. S.; Pople, J. A. *Gaussian98*; Gaussian, Inc.: Pittsburgh, PA, 1998.

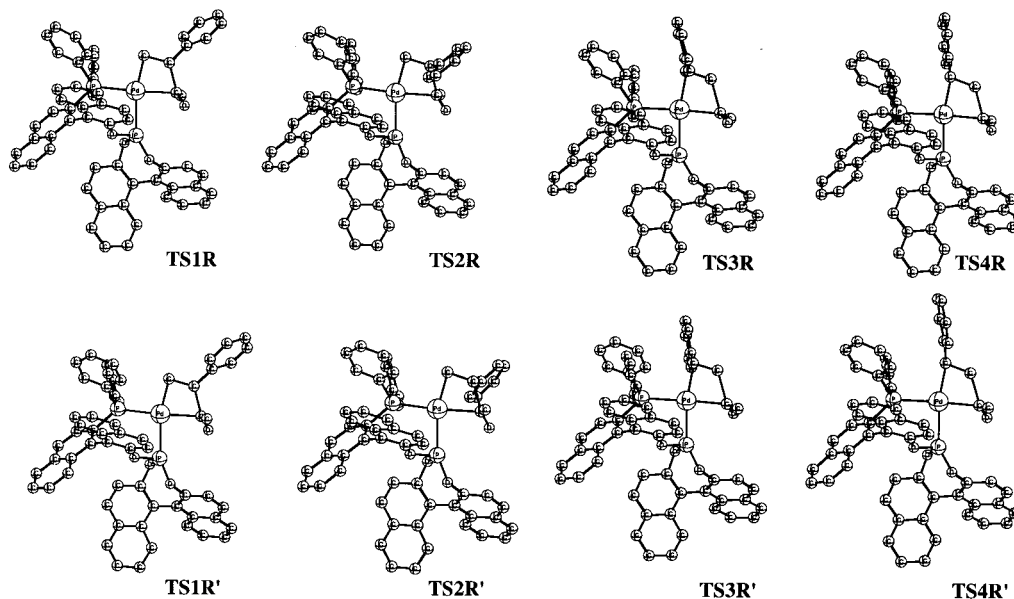


Figure 9. Optimized structures of the transition states in the 1,2- and 2,1-insertion of styrene into the acetyl-Pd bond with the combined MO + MM (B3LYP/lanl2dz + MM3) method. The real molecule was used. **TS1–4R** have the carbonyl oxygen oriented to the front, and **TS1–4R'** have the carbonyl oxygen oriented to the back. All hydrogen atoms are omitted for clarity. The calculated energies for all the structures are similar.

Table 1. Calculated Energies (in kcal/mol) at the B3LYP Level for the Optimized Structures of **TS1–4M** Relative to **TS1M**^a

	regioselectivity			
	1,2		2,1	
	TS1M	TS2M	TS3M	TS4M
B3LYP	0.0	−0.5	−6.8	−6.2

^a The basis set lanl2dz was used. See Figure 8 for the structures.

TSs obtained in the model molecule. Thus, on the basis of the orientation of carbonyl oxygen, each of the four diastereomers is accompanied by another diastereomer. Series of TSs **TS1–4R** have the carbonyl oxygen oriented to the front, and **TS1–4R'** have the carbonyl oxygen oriented to the back (Figure 9). The geometry optimizations were performed by the molecular mechanics (MM) method, MM3,¹⁹ for the eight diastereomeric TSs fixing the core part (Pd(P₂)(COMe)(C₂H₃)) at the corresponding geometries optimized at the B3LYP level in the model molecule, which is called the combined MO + MM (B3LYP + MM3) method.^{7b,20} In the MM3 calculations, for the Pd atom, the van der Waals parameters reported by Rappé et al. are used.²¹ The energies for the structures optimized with the combined MO + MM method were calculated by the ONIOM2 method using Pd(PH₃)(P(OH)₃)(COMe)(C₂H₃Ph) as a model system. As summarized in Table 2, the TSs for 1,2- and 2,1-insertions are almost equal in energy. This result shows a good agreement with the fact that the regio- and the enantioselectivities were rather low in the initial styrene insertion.

The contradicting results between the model and the real systems may be accounted for as follows. The MO calculation on the model system reflects the electronic requirement of the system. On the other hand, the calculation on the real molecule with the ONIOM method is influenced not only by electronic factors but also by steric factors. Thus, it seems that 2,1-insertion

Table 2. Calculated Energies (in kcal/mol) at Various ONIOM2 Levels for the Optimized Structures of **TS1–4R** and **TS1–4R'** Relative to **TS1R**^a

	regioselectivity			
	1,2		2,1	
	<i>R</i>	<i>S</i>	<i>R</i>	<i>S</i>
	TS1R	TS2R	TS3R	TS4R
ONIOM2(B3LYP:MM3)	0.0	−3.3	−4.4	−3.5
ONIOM2(B3LYP:HF)	0.0	−2.1	2.5	1.8
ONIOM2(B3LYP:B3LYP)	0.0	−3.5	1.2	0.8
	TS2R'	TS1R'	TS4R'	TS3R'
ONIOM2(B3LYP:MM3)	−2.8	−0.6	−0.7	−4.4
ONIOM2(B3LYP:HF)	−3.2	−3.1	1.4	−0.9
ONIOM2(B3LYP:B3LYP)	−2.7	−2.7	2.1	−0.3

^a The basis sets lanl2dz and lanl2mb were used for the B3LYP and HF calculations, respectively, in the ONIOM method. The model system used in the ONIOM2 calculations is Pd(PH₃)(P(OH)₃)(COMe)(C₂H₃Ph). See Figure 9 for the structures.

is favored electronically and that 1,2-insertion is favored sterically. As a consequence of the two factors, the initial styrene insertion resulted in low regioselectivity.

Preferable 1,2-Insertion in the Real Molecule: The Subsequent Insertions. In a procedure, the same as those for **TS1–4R** and **TS1–4R'**, the TSs for the second, the third, and the fourth styrene insertions were studied; those are as **TS1–4R-2** and **TS1–4R'-2**, **TS1–4R-3** and **TS1–4R'-3**, and **TS1–4R-4** and **TS1–4R'-4**, respectively. The structures were optimized with the combined MO + MM (B3LYP + MM3) method, and the energies were calculated by the ONIOM2 method for **TS1–4R-2** and **TS1–4R'-2** using Pd(PH₃)(P(OH)₃)(COMe)(C₂H₃Ph) as a model system and by the ONIOM3 method for **TS1–4R-3** and **TS1–4R'-3**, and for **TS1–4R-4** and **TS1–4R'-4** using Pd(PH₃)(P(OH)₃)(COMe)(C₂H₃Ph) as a small model system and Pd{(R,S)-BINAPHOS}(COC₂H₃-PhCOMe)(C₂H₃Ph) as an intermediate model system. The results are summarized in Table 3 and Figure 10. The energy of the TSs tend to be lower for 1,2-insertion than for 2,1-insertion in all insertions. This is in accordance to the experimental finding that the 1,2-insertion takes place predominantly. This

(19) Allinger, N. L. *mm3(92)*; QCPE: Bloomington, IN, 1992.

(20) (a) Kawamura-Kuribayashi, H.; Koga, N.; Morokuma, K. *J. Am. Chem. Soc.* **1992**, *114*, 8687. (b) Maseras, F.; Koga, N.; Morokuma, K. *Organometallics* **1994**, *13*, 4008.

(21) Rappé, A. K.; Casewit, C. J.; Colwell, K. S.; Goddard, W. A., III; Skiff, W. M. *J. Am. Chem. Soc.* **1992**, *114*, 10024.

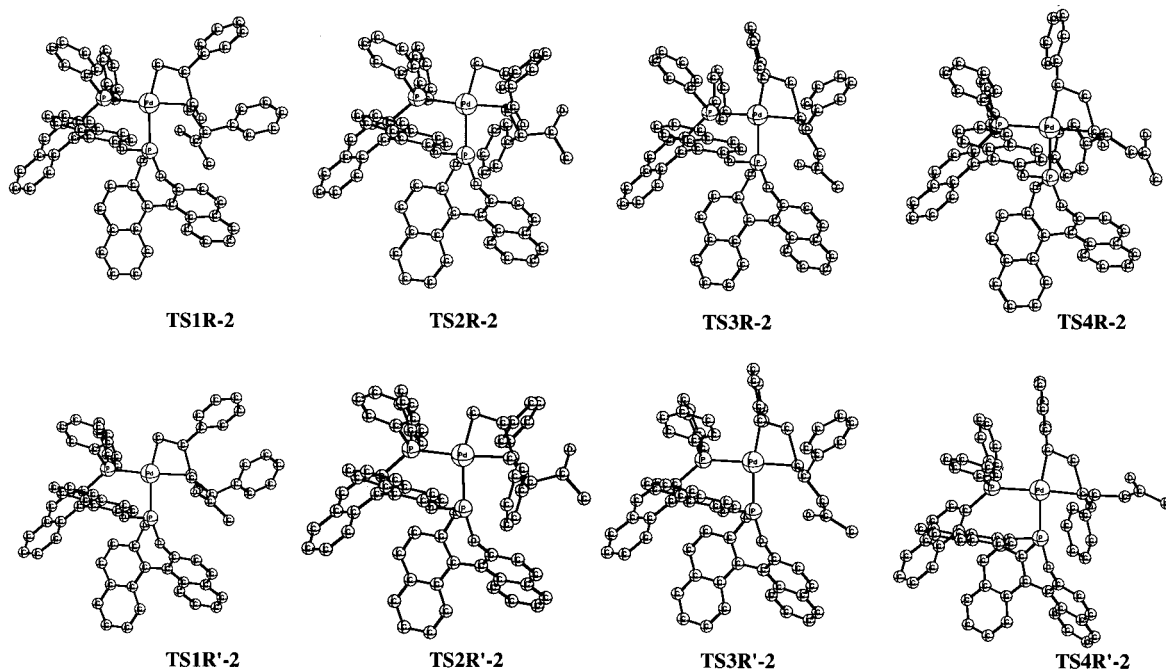


Figure 10. Optimized structures of the transition states in the 1,2- and 2,1-insertion of styrene into the acyl-Pd bond of $\text{CH}_3\text{CO}(\text{C}_2\text{H}_5\text{Ph})\text{CO-Pd}\{(R,S)\text{-BINAPHOS}\}$ with the combined MO + MM (B3LYP/lan12dz + MM3) method. **TS1-4R-2** and **TS1-4R'-2** correspond to **TS1-4R** and **TS1-4R'**, respectively. All hydrogen atoms are omitted for clarity.

Table 3. Calculated Energies (in kcal/mol) with the MM and ONIOM Methods for the Optimized Structures of **TS1-4R-2** and **TS1-4R'-2** Relative to **TS1R-2**; **TS1-4R-3** and **TS1-4R'-3** Relative to **TS1R-3**; and **TS1-4R-4** and **TS1-4R'-4** Relative to **TS1R-4**^a

	regioselectivity			
	1,2		2,1	
	R	S	R	S
	TS1R-2	TS2R-2	TS3R-2	TS4R-2
MM3	0.0	0.3	22.2	20.4
ONIOM2(B3LYP:HF)	0.0	0.5	6.7	10.8
	TS2R'-2	TS1R'-2	TS4R'-2	TS3R'-2
MM3	4.2	2.9	25.2	24.0
ONIOM2(B3LYP:HF)	-4.5	-5.3	10.7	4.9
	TS1R-3	TS2R-3	TS3R-3	TS4R-3
MM3	0.0	3.5	24.8	23.8
ONIOM3(B3LYP:HF:MM3)	0.0	5.6	10.9	21.3
	TS2R'-3	TS1R'-3	TS4R'-3	TS3R'-3
MM3	5.9	2.4	26.8	27.5
ONIOM3(B3LYP:HF:MM3)	0.8	-4.7	20.3	12.7
	TS1R-4	TS2R-4	TS3R-4	TS4R-4
MM3	0.0	3.8	24.9	23.8
ONIOM3(B3LYP:HF:MM3)	0.0	5.2	12.3	22.9
	TS2R'-4	TS1R'-4	TS4R'-4	TS3R'-4
MM3	6.4	3.0	30.0	27.5
ONIOM3(B3LYP:HF:MM3)	1.1	-3.4	16.3	14.6

^a The basis sets lan12dz and lan12mb were used for the B3LYP and HF calculations, respectively, in the ONIOM method. The model system used in the ONIOM2 calculations is $\text{Pd}(\text{PH}_3)(\text{P}(\text{OH})_3)(\text{COMe})(\text{C}_2\text{H}_5\text{Ph})$. The small model system and the intermediate model system used in the ONIOM 3 calculations are $\text{Pd}(\text{PH}_3)(\text{P}(\text{OH})_3)(\text{COMe})(\text{C}_2\text{H}_5\text{Ph})$ and $\text{Pd}\{(R,S)\text{-BINAPHOS}\}(\text{COC}_2\text{H}_5\text{PhCOMe})(\text{C}_2\text{H}_5\text{Ph})$, respectively. See Figure 10 and Supporting Information for the structures.

tendency may be interpreted on the basis of steric factors, although we could not specify any particular repulsive interactions responsible to the differentiation. Although the theoretical studies nicely explained the regioselectivity, the calculations do not fully match the experimental results with respect to enantioselectivity.

Conclusion

In conclusion, we have given evidence that supports 1,2-insertion for chain propagation and 2,1-insertion for chain termination. The rather unusual polymerization observed with Pd-BINAPHOS, as a phosphorus ligand system, may be attributed to the unique exclusive 1,2-insertion of styrene to the acyl-Pd bonds. This is in sharp contrast to the predominant 2,1-insertion with conventional nitrogen ligands.²⁻⁵ Theoretical studies suggested that the 1,2-insertion is derived from the steric demand of (R,S)-BINAPHOS rather than electronic demand. This steric requirement seems to increase as the polymer chain grows.

Meanwhile, when 2,1-insertion does take place, rapid β -hydride elimination occurs, as is common to the other phosphorus ligands, to terminate the polymerization. With the resulting Pd-H species, styrene inserts in a 2,1-fashion to give π -benzyl complexes which re-initiate the styrene-CO copolymerization.

Experimental Section

General. All manipulations involving the air- and moisture-sensitive compounds were carried out using standard Schlenk techniques under argon purified by passing through a hot column packed with BASF catalyst R3-11. All NMR spectra were recorded using JEOL EX-270 or Varian Mercury 200 spectrometers. Tetramethylsilane (¹H and ¹³C) and H₃PO₄ (³¹P) were employed as internal and external standards, respectively. Other characterization data were recorded by the use of the following instruments: gas chromatography (GLC), Shimadzu GC-15A equipped with a flame ionization detector; HPLC, TOSOH CCPM equipped with CO-8000 injection unit and UV-8000 detector; optical rotations, JASCO DIP-360; SEC, GL Sciences model 556 equipped with Showdex SE-61 RI detector and SIC GPC board; TOF mass spectroscopy, JEOL Voyager-DE STR. Melting points were measured on a Yanagimoto-Seisakusho micro melting point apparatus MP-500D and are uncorrected. Column chromatography was conducted on silica gel (Wakogel C-200) from Wako Pure Chemical Industries Ltd. Separation by GC was performed with a GL Science GC390 instrument. Elemental analyses were performed at the Microanalysis Center, Kyoto University. Most of the reagents were purchased from Wako Pure

Chemical Industries Ltd., Nacalai Tesque, or Aldrich Chemical Co., Inc., and were used without further purification unless otherwise specified. Solvents were purified by distillation under argon after drying over standard drying agents. Styrene which contains 0.003% of *tert*-butylcatechol was used without distillation. Carbon monoxide (99.9%) was obtained from Teisan Co. (*S*)-(-)-Binaphthol came from Sumikin Chemical Co. Ltd.

³¹P NMR Studies on the Regioselectivity of Styrene Insertion to Acetylpladium [Pd(COMe)(CD₃CN){(*R,S*)-BINAPHOS}]·[B{3,5-(CF₃)₂C₆H₃}]₄ (2) (See Also Figure 2). A solution of Pd(Me)(Cl)-{(R,S)-BINAPHOS} (23.8 mg, 0.0257 mmol) in CH₂Cl₂ (1.5 mL) was added to a solution of Na[B(3,5-(CF₃)₂C₆H₃)] (24.9 mg, 0.0281 mmol) in CD₃CN (0.5 mL). Deuterium-substituted acetonitrile was used for NMR studies in order to avoid a CH₃ peak in ¹H NMR. After the solution was stirred at 20 °C for 1 h, the solvents were removed in vacuo to give [Pd(Me)(CD₃CN){(*R,S*)-BINAPHOS}]·[B{3,5-(CF₃)₂C₆H₃}]₄ (1). The complex was dissolved in CDCl₃ (1.0 mL) and stirred under CO (1 atm) for 30 min to form acetylpladium 2. The solution was transferred into an NMR tube under 1 atm of CO atmosphere. Immediately after the addition of 3 equiv of styrene (0.009 mL, 0.0785 mmol), the NMR tube was placed in the NMR probe and cooled to -10 °C. After the tube was kept at -10 °C for 3 h, the ³¹P NMR spectrum showed the appearance of the 1,2-alkyl complex [Pd(CH₂-CHPhCOMe){(*R,S*)-BINAPHOS}]·[B{3,5-(CF₃)₂C₆H₃}]₄ (3a) and the 2,1-alkyl complex [Pd(CHPhCH₂COMe){(*R,S*)-BINAPHOS}]·[B{3,5-(CF₃)₂C₆H₃}]₄ (4). Upon warming of the solution to 20 °C, four new species appeared, which are assigned as 3b and 3c (diastereomers of 3a) and two π -benzyl complexes [Pd(η^3 -CH₃CHPh){(*R,S*)-BINAPHOS}]·[B{3,5-(CF₃)₂C₆H₃}]₄ (8a and 8b). After 44 h at 20 °C, 8a and 8b became the only visible species. The ³¹P NMR charts are summarized in Figure 2. **3a:** ³¹P NMR (CDCl₃ at 20 °C) δ 139.9 (d, $J_{P-P} = 64$ Hz), 14.6 (d, $J_{P-P} = 64$ Hz); (CDCl₃ at -10 °C) δ 140.9 (d, $J_{P-P} = 64$ Hz), 14.7 (d, $J_{P-P} = 64$ Hz). **3b:** ³¹P NMR (CDCl₃ at 20 °C) δ 149.9 (d, $J_{P-P} = 64$ Hz), 30.6 (d, $J_{P-P} = 67$ Hz); (CDCl₃ at -10 °C) δ 150.6 (d, $J_{P-P} = 67$ Hz), 31.7 (d, $J_{P-P} = 64$ Hz). **3c:** ³¹P NMR (CDCl₃ at 20 °C) δ 139.5 (d, $J_{P-P} = 64$ Hz), 14.9 (d, $J_{P-P} = 64$ Hz); (CDCl₃ at -10 °C) δ 140.5 (d, $J_{P-P} = 67$ Hz), 15.1 (d, $J_{P-P} = 64$ Hz). **4:** ³¹P NMR (CDCl₃ at 20 °C) δ 141.7 (d, $J_{P-P} = 98$ Hz), 19.1 (d, $J_{P-P} = 98$ Hz); (CDCl₃ at -10 °C) δ 141.9 (d, $J_{P-P} = 98$ Hz), 19.4 (d, $J_{P-P} = 98$ Hz). **8a:** ³¹P NMR (CDCl₃ at 20 °C) δ 152.4 (d, $J_{P-P} = 95$ Hz), 17.9 (d, $J_{P-P} = 95$ Hz); (CDCl₃ at -10 °C) δ 153.1 (d, $J_{P-P} = 95$ Hz), 17.9 (d, $J_{P-P} = 95$ Hz). **8b:** ³¹P NMR (CDCl₃ at 20 °C) δ 149.5 (d, $J_{P-P} = 98$ Hz), 17.5 (d, $J_{P-P} = 98$ Hz); (CDCl₃ at -10 °C) δ 150.3 (d, $J_{P-P} = 98$ Hz), 17.6 (d, $J_{P-P} = 98$ Hz). Assignment of the ³¹P NMR peaks to complexes 3, 4, and 8 was performed by repeating the same experiment using either ¹³C-labeled styrene (PhCH=¹³CH₂) or ¹³CO as shown in the next two paragraphs. ¹H NMR of the last sample showed the presence of 3-phenyl-3-buten-2-one (5)²¹ and 4-phenyl-3-buten-2-one (benzalacetone 6). ¹H NMR of 6 available from Aldrich: (CDCl₃ at 20 °C) δ 2.39 (s, 3H), 6.72 (d, $J = 16.5$ Hz, 1H), 7.36–7.43 (m, 3H), 7.46–7.59 (m, 3H). Because only the NMR data in CCl₄ were reported in the literature,²¹ we prepared 5 in order to compare the chemical shifts in CDCl₃. ¹H NMR of 3-phenyl-3-buten-2-one (5): (CDCl₃ at 20 °C) δ 2.45 (s, 3H), 5.97 (d, $J = 0.4$ Hz, 1H), 6.18 (d, $J = 0.5$ Hz, 1H), 7.25–7.40 (m, 5H).

NMR Data of 3, 4, and 8 with Styrene-2-¹³C (PhCH=¹³CH₂). **3a:** ³¹P NMR (CDCl₃ at 20 °C) δ 139.9 (dd, $J_{P-P} = 64$ Hz, $J_{P-C} = 6.1$ Hz), 14.6 (dd, $J_{P-P} = 64$ Hz, $J_{P-C} = 80$ Hz); ¹³C NMR (CDCl₃ at 20 °C) δ 39.3 (dd, $J_{P-C} = 80$ and 6.1 Hz). **3b:** ³¹P NMR (CDCl₃ at 20 °C) δ 149.9 (dd, $J_{P-P} = 64$ Hz, $J_{P-C} = 128$ Hz), 30.6 (dd, $J_{P-P} = 67$ Hz, $J_{P-C} = 3.1$ Hz); ¹³C NMR (CDCl₃ at 20 °C) δ 49.1 (dd, $J_{P-C} = 127$, 4.9 Hz). **3c:** ³¹P NMR (CDCl₃ at 20 °C) δ 139.5 (dd, $J_{P-P} = 64$ Hz, $J_{P-C} = 6.1$ Hz), 14.9 (dd, $J_{P-P} = 64$ Hz, $J_{P-C} = 79$ Hz); ¹³C NMR (CDCl₃ at 20 °C) δ 39.8 (dd, $J_{P-C} = 79$, 6.1 Hz). **4:** ³¹P NMR (CDCl₃ at 20 °C) δ 141.7 (d, $J_{P-P} = 98$ Hz), 19.1 (dd, $J_{P-P} = 98$ Hz, $J_{P-C} = 6.1$ Hz); ¹³C NMR (CDCl₃ at 20 °C) δ 51.8 (d, $J_{P-C} = 6.1$ Hz). **8a:** ³¹P NMR (CDCl₃ at 20 °C) δ 152.4 (d, $J_{P-P} = 95$ Hz), 17.9 (dd, $J_{P-P} = 95$ Hz, $J_{P-C} = 6.1$ Hz); ¹³C NMR (CDCl₃ at 20 °C) δ 16.2 (d, $J_{P-C} = 6.1$ Hz, CH₃ by DEPT). **8b:** ³¹P NMR (CDCl₃ at 20 °C) δ 149.5 (d, $J_{P-P} = 98$ Hz), 17.5 (dd, $J_{P-P} = 98$ Hz, $J_{P-C} = 6.1$ Hz); ¹³C NMR (CDCl₃ at 20 °C) δ 18.5 (d, $J_{P-C} = 6.1$ Hz, CH₃ by DEPT).

NMR Data of 3a, 4, and 8a with ¹³CO. **3a:** ³¹P NMR (CDCl₃ at 20 °C) δ 139.9 (d, $J_{P-P} = 64$ Hz), 14.6 (dd, $J_{P-P} = 64$ Hz, $J_{P-C} = 11$ Hz); ¹³C NMR (CDCl₃ at 20 °C) δ 237.7 (dd, $J_{P-C} = 11$ Hz, $J_{Pb-C} = 2.4$ Hz). **3b:** ¹³C NMR (CDCl₃ at 20 °C) δ 236.7 (dd, $J_{P-C} = 2.4$ Hz, $J_{Pb-C} = 11$ Hz). **3c:** ¹³C NMR (CDCl₃ at 20 °C) δ 237.1 (dd, $J_{P-C} = 9.8$ Hz, $J_{Pb-C} = 2.4$ Hz). **4:** ³¹P NMR (CDCl₃ at 20 °C) δ 141.7 (d, $J_{P-P} = 98$ Hz), 19.1 (dd, $J_{P-P} = 98$ Hz, $J_{P-C} = 12$ Hz); ¹³C NMR (CDCl₃ at 20 °C) δ 224.1 (dd, $J_{P-C} = 12$ Hz, $J_{Pb-C} = 3.6$ Hz). **8a:** ³¹P NMR (CDCl₃ at 20 °C) δ 152.4 (d, $J_{P-P} = 95$ Hz), 17.9 (d, $J_{P-P} = 95$ Hz), no J_{P-C} was observed. **8b:** ³¹P NMR (CDCl₃ at 20 °C) δ 149.5 (d, $J_{P-P} = 98$ Hz), 17.5 (d, $J_{P-P} = 98$ Hz), no J_{P-C} was observed.

Preparation of the Authentic Sample of 1,2-Ester 14. First, methyl 3-phenyl-4-pentenoate (18) was prepared. A mixture of cinnamyl alcohol (17, 10.2 g, 76.5 mmol) with 1.5 equiv of trimethyl orthoacetate (15 mL, 117 mmol) and 0.04 equiv of propionic acid (0.4 mL, 5.36 mmol) was gradually heated to 140 °C and then kept at 140–150 °C for 21 h. Water was added to the reaction mixture, and the aqueous layer was extracted with ether. The combined organic layers were washed with saturated aqueous NaHCO₃ and saturated aqueous NaCl, dried over magnesium sulfate, and concentrated under reduced pressure to give methyl 3-phenyl-4-pentenoate (18) as the crude product (ca. 82% yield). The terminal C–C double bond was transformed into an acetyl group via a Wacker process. A mixture of PdCl₂ (1.12 g, 6.33 mmol) and CuCl (6.24 g, 63.1 mmol) in aqueous dimethylformamide (DMF/H₂O = 7/1, total 50 mL) was stirred under an oxygen balloon at room temperature for 2.5 h until the suspension turned a green-brown color. Crude 18 (12 g, 62.8 mmol), obtained above, was added within 20 min by additional funnel, accompanied by vigorous stirring under an oxygen balloon at room temperature. The solution turned green-brown to black within 20 min and then returned gradually to green-brown. After being stirred for 4 days, the mixture was poured into aqueous 1 M HCl and extracted with diethyl ether. The combined organic layers were washed with saturated aqueous NaHCO₃ and saturated aqueous NaCl, dried over magnesium sulfate, and concentrated under a reduced pressure. The crude product was purified by distillation (89–90 °C, 0.7 Torr) to give methyl 3-phenyl-4-oxopentanoate (14, 2.61 g, 12.7 mmol) in 20% yield: ¹H NMR (CDCl₃, at 20 °C) δ 2.12 (s, 3H), 2.53 (dd, $J_{H-H} = 16.8$, 5.0 Hz, 1H), 3.22 (dd, $J_{H-H} = 16.8$, 9.8 Hz, 1H), 3.65 (s, 3H), 4.19 (dd, $J_{H-H} = 9.7$, 5.0 Hz, 1H), 7.2–7.4 (m, 5H); ¹³C NMR (CDCl₃, at 20 °C) δ 28.8, 36.7, 51.7, 54.8, 127.7, 128.2, 129.1, 137.3, 172.5, 206.8; IR (neat) 1733, 1715, 1595, 1490 cm⁻¹. Elemental analysis, calcd for C₁₂H₁₄O₃: C, 69.89; H, 6.84. Found: C, 69.81; H, 6.93.

Hydrolysis of Ester 14 to Acid 19. A mixture of methyl ester 14 (711 mg, 3.45 mmol) with KOH, MeOH, and H₂O was stirred for 1 h at room temperature. The mixture was poured into aqueous 1 M HCl and extracted with ether. The combined organic layers were washed with saturated aqueous NaCl, dried over magnesium sulfate, and concentrated under reduced pressure to give 19 quantitatively: ¹H NMR (DMSO-*d*₆, at 20 °C) δ 2.02 (s, 3H), 2.45 (dd, $J_{H-H} = 16.9$, 5.3 Hz, 1H), 2.99 (dd, $J_{H-H} = 16.9$, 9.9 Hz, 1H), 4.18 (dd, $J_{H-H} = 9.7$, 4.9 Hz, 1H), 7.22–7.43 (m, 5H), 12.23 (s, 1H); ¹³C NMR (DMSO-*d*₆, at 20 °C) δ 28.1, 36.5, 53.8, 127.4, 128.2, 128.9, 131.8, 172.8, 206.8; IR (Nujol) 3400–2700, 1730, 1685 cm⁻¹. Elemental analysis, calcd for C₁₁H₁₂O₃: C, 68.74; H, 6.29. Found: C, 68.53; H, 6.34.

Optical Resolution of 19 by Preferential Crystallization with (*R*)-(+)-Phenethylamine. Acid 19 (301 mg, 1.57 mmol) was dissolved in *i*-PrOH (1.5 mL). To the solution was added 1.04 equiv of (*R*)-(+)-1-phenethylamine (0.21 mL, 1.63 mmol), and the solution was heated. The solution was cooled to room temperature and allowed to stand for 24 h. The resulting colorless solids were collected by filtration, washed with drops of *i*-PrOH, and dried to give (-)-CH₃COCHPhCH₂COO⁻·(*R*)-(+)-1-phenethylammonium salts as colorless solids (305 mg, 0.975 mmol). The salts were neutralized with aqueous 6 M HCl, and the carboxylic acid was extracted with ether. Removal of the solvent afforded (*R*)-(-)-19 (124 mg, 0.643 mmol) with 27% ee (determined by gas chromatography using a chiral column, Chrompak, CP-Cyclodextrin- β -236M, 159 °C). [α]_D²⁰ = -167.55 (*c* 0.45, CHCl₃). The absolute configuration was determined to be *R* by comparing the optical rotation with related compounds (see Figure 4).

Determination of the Absolute Configuration of Ester 14. The above-prepared (*R*)-(-)-**19** (27% ee, 124 mg, 0.643 mmol) was dissolved in H₂SO₄/MeOH and refluxed for 1 h. The mixture was poured into water and extracted with ether. The combined organic layers were washed with saturated aqueous NaHCO₃ and saturated aqueous NaCl, dried over sodium sulfate, and concentrated in vacuo. The crude product was purified by silica gel chromatography (hexane/ethyl acetate = 2/1) to give (*R*)-(-)-**14** (94.6 g, 0.459 mmol). The enantiomeric excess (31% ee) was determined by HPLC (Chiralcel OJ, hexane/*i*-PrOH = 9/1, *t_R* = 14.5 min (*S*), 16.0 min (*R*)). [α]_D²⁰ = -1.66 (*c* 0.48, CHCl₃). The absolute configuration was again confirmed by comparing the optical rotation with those of related compounds (see Figure 4). The major enantiomer is *R*, in agreement with the characterization of the acid in the previous paragraph.

Preparation of an Authentic Sample of 2,1-Ester 15. First, methyl 2-phenyl-4-pentenoate (**21**) was prepared. To a solution of diisopropylamine (3.6 mL, 25.7 mmol) in THF (50 mL) was added butyllithium (1.45 M, 16.5 mL, 23.9 mmol) at 0 °C, and then the solution was stirred at 0 °C for 30 min to prepare LDA. After the solution was cooled to -78 °C, methyl phenylacetate (2.9 mL, 20.2 mmol) in THF (20 mL) was added within 5 min. The solution was stirred at -78 °C for 1.5 h, and HMPA (7 mL, 40.2 mmol) and then allyl bromide (3.5 mL, 40.4 mmol) were added. After being stirred at -78 °C for 1 h, the mixture was poured into saturated aqueous NH₄Cl and extracted with ether. The combined organic layers were washed with saturated aqueous NaHCO₃ and saturated aqueous NaCl, dried with magnesium sulfate, and concentrated under reduced pressure to give methyl 2-phenyl-4-pentenoate (**21**, 4.27 g) as a crude product (ca. 94% yield). The olefinic bond of **21** was oxidized by the Wacker reaction as was done for 1,2-product **18** (vide supra). Purification by silica gel chromatography (hexane/ethyl acetate = 3/1) and recrystallization with hexane gave methyl 2-phenyl-4-oxopentanoate (**15**, 2.44 g, 11.8 mmol, 52% from **21**): ¹H NMR (CDCl₃, at 20 °C) δ 2.18 (s, 3H), 2.71 (dd, *J_{H-H}* = 18.0, 4.2 Hz, 1H), 3.40 (dd, *J_{H-H}* = 18.0, 10.4 Hz, 1H), 3.66 (s, 3H), 4.11 (dd, *J_{H-H}* = 10.4, 4.2 Hz, 1H), 7.2–7.4 (m, 5H); ¹³C NMR (CDCl₃, at 20 °C) δ 29.9, 46.0, 47.1, 52.3, 127.5, 127.7, 128.8, 138.0, 173.7, 206.2; IR (neat) 1730, 1715, 1600, 1495 cm⁻¹. Elemental analysis, calcd for C₁₂H₁₄O₃: C, 69.89; H, 6.84. Found: C, 69.66; H, 6.98.

Hydrolysis of Ester 15 to Acid 22. Hydrolysis of ester **15** (0.888 g, 4.30 mmol) with KOH, MeOH (20 mL), and H₂O (10 mL) gave **22** in 95% yield (0.786 g, 4.09 mmol): ¹H NMR (DMSO-*d*₆, at 20 °C) δ 2.08 (s, 3H), 2.73 (dd, *J_{H-H}* = 18.1, 4.3 Hz, 1H), 3.24 (dd, *J_{H-H}* = 18.1, 10.6 Hz, 1H), 3.87 (dd, *J_{H-H}* = 10.6, 4.3 Hz, 1H), 7.18–7.46 (m, 5H), 12.34 (s, 1H); ¹³C NMR (DMSO-*d*₆, at 20 °C) δ 29.6, 45.8, 46.3, 127.1, 127.7, 128.6, 138.9, 174.1, 206.4; IR (Nujol) 3400–2400, 1710, 1690 cm⁻¹. Elemental analysis, calcd for C₁₁H₁₂O₃: C, 68.74; H, 6.29. Found: C, 68.47; H, 6.33.

Optical Resolution of 22 by Preferential Crystallization of Their Racemic Salts. To a solution of acid **22** (145 mg, 0.756 mmol) in *i*-PrOH (0.7 mL) was added 1.1 equiv of (*S*)-(-)-1-(2-naphthyl)ethylamine (0.13 mL, 0.804 mmol), and the mixture was heated. The solution was cooled to room temperature and allowed to stand for 24 h. Precipitated colorless solids were collected by filtration, washed with a small amount of *i*-PrOH, and dried in vacuo to give CH₃COCH₂-CHPhCOO⁻(*S*)-(-)-naphthylethylammonium salts as colorless solids. Acid (*R*)-**22** was obtained by neutralization with aqueous 1 M HCl with a trace contamination of (*S*)-(-)-naphthylethylamine. The absolute configuration and the enantiomeric excess were determined after esterification as described in the next paragraph.

Determination of the Absolute Configuration of 15. A solution of (*R*)-**22** in H₂SO₄ and MeOH was refluxed for 1 h. The mixture was poured into water and extracted with ether. The combined organic layers were washed with saturated aqueous NaHCO₃ and saturated aqueous NaCl, dried over sodium sulfate, and concentrated under reduced pressure. The crude product was purified by silica gel chromatography (hexane/ethyl acetate = 2/1) to give (*R*)-**15** (15.1 mg, 0.0732 mmol). The enantiomeric excess (71% ee) was determined by HPLC (Chiralcel OJ, hexane/*i*-PrOH = 9/1, 22 min (*S*) and 25 min (*R*)). [α]_D²⁰ = -108.76 (*c* 0.79, CHCl₃). The absolute configuration was determined by comparing the optical rotation with those of related compounds (see Figure 4).

Carbomethoxylation of Alkyl Complexes 3, 4, and 8. A solution of acetylpladium **2** in CH₂Cl₂ (4 mL) was prepared from Pd(Me)(Cl){(*R,S*)-BINAPHOS} (81.1 mg, 0.0875 mmol) and Na[B(3,5-(CF₃)₂C₆H₃)] (84.8 mg, 0.0956 mmol) as described above. To this, styrene (0.030 mL, 0.261 mmol) was added and stirred for 2 h at 20 °C. The solution were stripped of the solvents to give a mixture of 1,2-alkyl complex **3a–c**, 2,1-alkyl complex **4**, and π -benzyl complex **8a,b**: **3/4/8** = 48/20/16 (determined by ³¹P NMR). One additional species (16%) was characterized as methylpladium **1**, produced by decarbonylation from acyl complex **2**. The crude mixture was dissolved in CH₂Cl₂ (4 mL) and methanol (2 mL). The solution was degassed by three cycles of freeze–thaw, transferred into a 50-mL autoclave, and stirred under CO (20 atm) at 20 °C for 17 h. The residual Pd species were removed by silica gel column chromatography (hexane/ethyl acetate = 3/1). Four kinds of organic molecules were obtained after separation by GC (SE30, 150 °C, *t_R* = 38 min). CH₃COCHPhCH₂-COOCH₃ (**14**, 1,2-product from **3**): 11% yield based on Pd, 67% ee *S* (determined by HPLC, Chiralcel OJ, hexane/*i*-PrOH = 9/1, *t_R* = 14.3 min (*S*), 15.8 min (*R*)). CH₃COCH₂CHPhCOOCH₃ (**15**, 2,1-product from **4**): 4% yield based on Pd, 88% ee *S* (Chiralcel OJ, hexane/*i*-PrOH = 9/1, *t_R* = 21.9 min (*S*) and 24.9 min (*R*)). CH₃CHPhCOOCH₃ (**16**, from π -benzyl **8**): 3% yield based on Pd, 74% ee *S* (determined by HPLC, Chiralcel OJ, hexane/*i*-PrOH = 99.5/0.5, *t_R* = 16.1 min (*S*), 25.2 min (*R*)), absolute configuration was determined by comparison of the optical rotation with that of the commercially available sample from Aldrich. CH₃COCH=CHPh (**6**, from **4** by β -hydride elimination): 4% yield based on Pd.

³¹P NMR Studies on Styrene Insertion to Polymer-Attached Complex 29. First, the palladium complex bearing a polymer chain (complex **29**) was prepared. A solution of **1** in CDCl₃ (2.0 mL) was prepared from Pd(Me)(Cl){(*R,S*)-BINAPHOS} (38.0 mg, 0.0410 mmol) and Na[B{3,5-(CF₃)₂C₆H₃}]₄ (36.4 mg, 0.0410 mmol) and transferred into a 50-mL autoclave. The solution was stirred under partial pressures of propene (3 atm, 6.24 mmol) and CO (20 atm) at 20 °C for 15 min. After the pressure was released, formation of alkylpladium [Pd{(*R,S*)-BINAPHOS}(CH₂CHMeCO(CH₂CHMeCO)_{*n*}Me)·[B{3,5-(CF₃)₂C₆H₃}]₄] (**29**) was confirmed by ³¹P NMR: (CDCl₃, at 20 °C) δ 140.7 (d, *J_{P-P}* = 66 Hz), 13.4 (d, *J_{P-P}* = 66 Hz). The values are identical to the ones previously reported for [Pd{(*R,S*)-BINAPHOS}(CH₂-CHMeCO)_{*n*}Me]·[B{3,5-(CF₃)₂C₆H₃}]₄.^{7b} To estimate the polymer size, an aliquot of the solution was quenched by carbomethoxylation for SEC analysis using polystyrene as a standard: *M_n* = 1000 (*M_w*/*M_n* = 1.1), degree of polymerization ~14. The solution of **29** in CDCl₃ (2 mL) was bubbled with CO to remove the residual propene. Three equivalents of styrene (0.014 mL) was added, and the mixture was stirred under CO (20 atm) at -20 °C for 15 h. After the pressure was released, a part of the solution was transferred into an NMR tube for ³¹P NMR measurement. The spectrum showed the appearance of a new species which has been assigned as [Pd(CH₂CHPhCO(CH₂CHMeCO)_{*n*}Me){(*R,S*)-BINAPHOS}]·[B(3,5-(CF₃)₂C₆H₃)]₄ (*n* ≈ 14) (**30**): ³¹P NMR (CDCl₃, at 20 °C) δ 139.8 (d, *J_{P-P}* = 67 Hz), 14.3 (d, *J_{P-P}* = 67 Hz). **With Styrene-2-¹³C:** ³¹P NMR (CDCl₃, at 20 °C) δ 139.8 (d, *J_{P-P}* = 67 Hz), 14.3 (dd, *J_{P-P}* = 67 Hz, *J_{P-C}* = 80 Hz). No other peaks were affected by the ¹³C-labeling.

Copolymerization of Styrene and CO Initiated by 1. A solution of **1** in CH₂Cl₂ (2 mL), prepared from Pd(Me)(Cl){(*R,S*)-BINAPHOS} (9.3 mg, 0.010 mmol) and Na[B(3,5-(CF₃)₂C₆H₃)] (9.8 mg, 0.011 mmol), was transferred into a 50-mL autoclave. To this was added styrene (0.57 mL, 4.97 mmol), and the mixture was stirred under CO (20 atm) at 20 °C for 24 h. The mixture was poured into MeOH to precipitate poly(styrene-*alt*-CO) (105.2 mg, 16% yield): ¹H NMR (CDCl₃, at 20 °C) δ 6.96–7.53, 3.87–3.92, 3.07–3.18, 2.55–2.63 (Figure 6). The chain end was observed at δ 6.66 (d) for (*E*)-PhCH=CHCO—. On the basis of the integration, the molecular weight of the polymer was calculated to be 1800. ¹³C NMR (CDCl₃; *d*²-HFIP = 1:1, 20 °C) δ 210.3, 136.5, 129.3, 128.3, 127.7, 52.9, 44.9 (Figure 1). Molecular weight *M_n* = 2300 (*M_w*/*M_n* = 1.4) was estimated by SEC using a polystyrene standard (Shodex, KF-804L, THF as an eluate). The molecular weight is smaller than the value obtained with 4-*tert*-butylstyrene-CO, *M_n* = 5600 (*M_w*/*M_n* = 1.3), under the same reaction condition as the current styrene-CO. [Φ]_D²⁰ = -344.09 (*c* 0.50,

CHCl₃). MALDI-TOF mass spectroscopy showed the existence of two series of polymers, PhCH=CHCO(CH₂CHPhCO)_nMe and PhCH=CHCO(CH₂CHPhCO)_nCHMePh (Figure 7).

Acknowledgment. We are grateful to Profs. M. Sawamoto and M. Kamigaito (Kyoto University) for the measurement of MALDI-TOF mass spectroscopy. Part of the calculations was carried out at the Computer Center of the Institute for Molecular Science, Japan. We acknowledge financial support from the Ministry of Education, Science, Sports and Culture, Japan; for T.H. by a Grant-in-Aid for COE Research on Elements Science,

No. 12CE2005; and for K.N. and T.M. by a Grant-in-Aid for Scientific Priority Area "Molecular Physical Chemistry" (No. 403). We thank the Japan Society for the Promotion of Science (JSPS) for the financial support to Y.K.

Supporting Information Available: Optimized structures of CH₃CO(C₂H₃Ph)_nCO-Pd{(R,S)-BINAPHOS} for *n* = 2 and 3 (PDF). This material is available free of charge via the Internet at <http://pubs.acs.org>.

JA001395P